

Kinetics of Dissociative Electron Transfer to Ascaridole and Dihydroascaridole—Model Bicyclic Endoperoxides of Biological Relevance

Robert L. Donkers and Mark S. Workentin*^[a]

Abstract: The homogeneous and heterogeneous electron transfer (ET) reduction of ascaridole (**ASC**) and dihydroascaridole (**DASC**), two bicyclic endoperoxides, chosen as convenient models of the bridged bicyclic endoperoxides found in biologically relevant systems, were studied in aprotic media by using electrochemical methods. ET is shown to follow a concerted dissociative mechanism that leads to the distonic radical anion, which is itself reduced in a second step by an overall two-electron process. The kinetics of homogeneous ET to these endoperoxides from an extensive series of radical anion electron donors were measured as a function of the driving force of electron transfer ($\Delta G_{\text{ET}}^{\circ}$). The kinetics of heterogeneous

ET were also studied by convolution analysis. Together, the heterogeneous and homogeneous ET kinetic data provide the best example of the parabolic nature of the activation–driving force relationship for a concerted dissociative ET described by Savéant; the data is particularly illustrative due to the low bond-dissociation enthalpy (BDE) of the O–O bond and hence small intrinsic barriers. Analysis of the data allowed the dissociative reduction potentials (E_{diss}°) to be determined as -1.2 and -1.1 V against SCE for **ASC** and **DASC**,

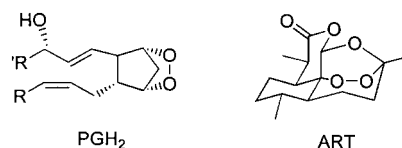
Keywords: electrochemistry • electron transfer • endoperoxides • O–O activation • radical ions

respectively. Unusually low pre-exponential factors measured in temperature-dependent kinetic studies suggest that ET to these O–O bonded systems is nonadiabatic. Analysis of ET kinetics for **ASC** and **DASC** by the Savéant model with a modification for nonadiabaticity allowed the intrinsic free energy for ET to be determined. The use of this approach and estimates for the BDE provide approximations of the reorganization energies. We suggest the methodology described herein can be used to evaluate the extent of ET to other endoperoxides of biological relevance and to provide thermochemical data not otherwise available.

Introduction

Endoperoxides are compounds whose oxygen–oxygen (O–O) bond often plays a key role in the activity of a number of chemically and biologically relevant substances.^[1, 2] Recent reviews summarize the numerous marine and terrestrial sources of endoperoxides that exhibit wide-ranging bioactivity, with many targeted as drug candidates.^[1, 2] An important example of an endoperoxide found in vivo is the prostaglandin endoperoxide (**PGH₂**), a key intermediate in the biosynthesis of fatty acids to prostaglandins, prostacyclins, thromboxanes and leukotrienes.^[3] Another example that has been well publicized is the potent antimalarial 1,2,4-trioxane,

artemisinin (**ART**), and related semisynthetic derivatives.^[4–21] It has only recently been generally agreed that the mechanism of antimalarial action involves an initial heme Fe(II)-mediated electron transfer (ET), which leads to fragmentation of the endoperoxide O–O bond. This results in the formation of oxygen-centered radical intermediates, which subsequently lead to the toxic intermediates.^[20, 22–29]



[a] Prof. M. S. Workentin, Dr. R. L. Donkers
Department of Chemistry, University of Western Ontario
London, Ontario N6A 5B7 (Canada)
Fax: (+1) 519-661-3022
E-mail: mworkent@uwo.ca

Supporting information for this article is available on the WWW under <http://www.wiley-vch.de/home/chemistry/> or from the author. A complete description of the temperature dependent rate studies, including plots of the data and tables of the experimental and calculated activation parameters.

ET reduction of O–O bonds in acyclic peroxides, α -peroxy lactones, α -pyrone endoperoxides, and dioxetanes is also recognized in connection with the chemically initiated electron-exchange luminescence (CIEEL) mechanism.^[30–37] Although a generally accepted mechanism is yet to be established,^[38–42] the ET to the O–O bond in CIEEL is described essentially as a concerted dissociative process. However, little

other insight into the fine detail of the ET mechanism has been provided. In contrast, and with few exceptions,^[1, 3, 43, 44] ET is not generally considered in the mechanism of action of endoperoxides; this is due, in part, to the lack of accurate thermodynamic and kinetic information on these types of systems. Proper consideration of the role of ET in the possible modes of action requires knowledge of the driving force for ET between the donor and the endoperoxide. Without accurate values of the standard reduction potential of each, the feasibility of ET cannot be determined accurately. This represents the most difficult challenge with these molecular systems.

Based on work by others^[45, 46] and ourselves^[47, 48] on the reduction of acyclic peroxides, the ET reduction mechanism of the O–O bond in endoperoxides should be concerted dissociative, in which bond fragmentation and electron uptake occur in a single step. For endoperoxides,^[49–51] ET and O–O cleavage lead to the concerted formation of an intermediate that we refer to as a distonic radical anion [Eq. (1)], in which charge and spin are separated.



In Equation (1) the electron (e^-) source can either be an electrode (heterogeneous) or a homogeneous reactant. Reduction potentials for concerted dissociative processes are not easily determined by using simple heterogeneous electrochemical methods, since the direct reduction is subject to a large over-potential due to the slow, rate-determining heterogeneous ET. When the standard reduction potentials cannot be conveniently measured, they can often be estimated by using thermochemical cycles.^[52] However, unlike many acyclic peroxides, the data required in the thermochemical cycles for endoperoxides are not readily available from thermolysis studies.^[53–55] In order to determine these thermochemical parameters that aid in understanding the mechanism of action of endoperoxides, and to better understand the chemistry that could be initiated by ET, we began a detailed investigation into the kinetics of ET chemistry to endoperoxides using electrochemical techniques.

The rate constant for ET, k_{ET} , is related to the reaction activation free energy, ΔG^\ddagger , by Equation (2), in which κ_{el} is the transmission coefficient and Z is a pre-exponential term.

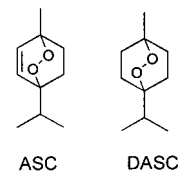
$$k_{\text{el}} = \kappa_{\text{el}} Z \exp\left(\frac{-\Delta G^\ddagger}{RT}\right) \quad (2)$$

Over the last decade, Savéant and co-workers have provided a framework that allows the kinetics of ET to be predicted for concerted dissociative reductions.^[56–58] Savéant's model relates the activation free energy, ΔG^\ddagger , to the reaction free energy, ΔG° , by an equation similar to the well-known Marcus equation [Eq. (3)], except that the intrinsic barrier, ΔG_0^\ddagger , contains contributions from the bond dissociation enthalpy (BDE) of the fragmenting bond in addition to the reorganization energy, λ [Eq. (4)].

$$\Delta G^\ddagger = \Delta G_0^\ddagger \left(1 + \frac{\Delta G^\circ}{4\Delta G_0^\ddagger}\right)^2 \quad (3)$$

$$\Delta G_0^\ddagger = \frac{\lambda + \text{BDE}}{4} \left(1 + \frac{\Delta G^\circ}{\lambda + \text{BDE}}\right)^2 \quad (4)$$

Examining the kinetics of ET and utilizing Savéant's model can provide important thermochemical parameters. The model was successfully applied to studying the dissociative reduction of the C–X bonds of alkyl and benzyl halides,^[59–63] N–X,^[64] C–S,^[65, 66] and S–S^[67, 68] bonds. Considerably fewer studies have been done on the reduction of the O–O bonds of peroxides.^[46–48, 51] In a preliminary communication we reported the only known estimates of the standard dissociative reduction potentials (E_{diss}°) of any endoperoxide, specifically two bicyclic endoperoxides, ascaridole (**ASC**) and dihydroascaridole (**DASC**) using this approach.^[51] **ASC** is a natural product with known activity as an anthelmintic,^[69] but it was chosen, along with **DASC**, as a suitable model system for the broader class of bioactive endoperoxides, such as **PGH₂**. Our analysis in the preliminary report involved examining the kinetics of the homogeneous electron-transfer reduction of these endoperoxides as a function of the potential of the electron donor.



We now report the complete details of this kinetic study, including an investigation of the temperature dependence of the rate constants, and the determination of heterogeneous rate constants from electrochemical data by using convolution potential sweep voltammetry. Together, the heterogeneous and homogeneous ET data provide the most comprehensive study of the kinetics of ET to endoperoxides. Our results show that ET to the O–O bond is nonadiabatic. These kinetic and mechanistic details have important ramifications to understanding ET to the O–O bonds in endoperoxides in vivo. More fundamentally, **ASC** and **DASC** also provide unique and interesting cases for studying dissociative ET because, unlike previous examples, the anion product in the dissociative reduction remains in the same molecule. The systems described here provide an unprecedented example of the parabolic activation–driving force relationship observed for dissociative ET systems, presumably because of the low O–O BDE and thus low intrinsic barrier.

Results and Discussion

Cyclic voltammetry and coulometry: Cyclic voltammetry was used to study the reduction of **ASC** and **DASC** in both acetonitrile (MeCN) and *N,N*-dimethylformamide (DMF) containing 0.1M tetraethylammonium perchlorate (TEAP) at 25 °C with a glassy carbon cathode. A representative cyclic voltammogram of **ASC** measured under these conditions is shown in Figure 1. The voltammograms of both **ASC** and **DASC** are essentially identical and show a broad, irreversible cathodic peak at all the potential scan rates investigated (0.1 to 50 Vs^{-1}). At 0.1 Vs^{-1} , the peak potentials (E_p) of the reduction of **ASC** and **DASC** are –1.85 and –1.90 V against SCE in MeCN, respectively, and –1.88 and –1.93 V against SCE in DMF. On glassy carbon the voltammograms are reproducible, and the position and shape of the reduction waves do not change in the presence of non-nucleophilic acids

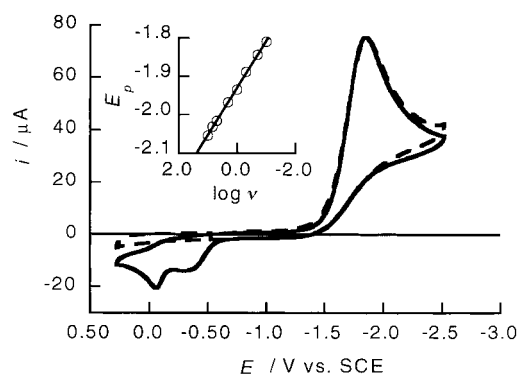


Figure 1. Cyclic voltammograms at 0.2 V s^{-1} in ACN with 0.1 mol L^{-1} TEAP for 2 mmol L^{-1} **ASC**. Dashed lines show the presence of excess 2,2,2-trifluoroethanol. Inset: plot of the dependence of the peak potential as a function of scan rate.

such as 2,2,2-trifluoroethanol (TFE; shown in Figure 1) or acetanilide. Irreversible anodic peaks are also observed for **ASC** and **DASC**; the peak current depending on the scan rate. The position of these peaks and the observation that they disappear in the presence of acid indicate that they are due to the oxidation of alkoxides formed in the initial reduction and/or other electro-generated bases. Increasing the potential scan rate, ν , causes the E_p to become more negative by an average value of $123 \text{ mV} (\log \nu)^{-1}$ (Figure 1, inset) for both **ASC** and **DASC**. The peak width, defined as the difference between the potential at the half-current height and peak potential (i.e., $\Delta E_{p/2} = E_{p/2} - E_p$), of the reduction wave also varies by scan rate. For **ASC**, the $\Delta E_{p/2}$ is 182 mV at 0.2 V s^{-1} , and increases to 203 mV at 10 V s^{-1} . A summary of the voltammetric data of these two compounds appears in Table 1 and indicates a potential dependence on the transfer coefficient, α .^[56, 70]

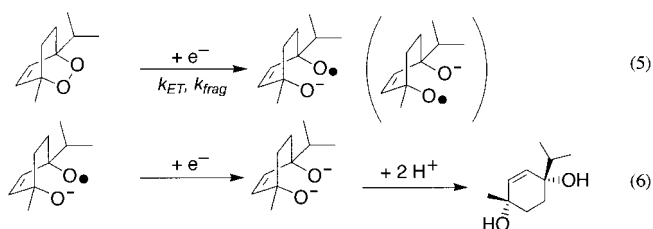
Table 1. Voltammetric data for the reduction of **ASC** and **DASC** in DMF and MeCN (0.1 M TEAP) at 25°C measured by cyclic voltammetry at a glassy carbon working electrode.

		MeCN		DMF	
		ASC	DASC	ASC	DASC
E_p (V versus SCE)	0.1 V s^{-1}	-1.85	-1.90	-1.88	-1.93
	1.0 V s^{-1}	-1.97	-2.00	-1.98	-2.06
	10 V s^{-1}	-2.12	-2.11	-2.16	-2.23
$\alpha_{\text{app}} = -(RT/nF)(d \ln \nu / dE)$		0.24	0.24	0.24	0.24
$\alpha = 1.85 RT / F(E_{p/2} - E_p)$	0.1 V s^{-1}	0.267	0.270	0.285	0.270
	1.0 V s^{-1}	0.253	0.254	0.259	0.253
	10 V s^{-1}	0.234	0.236	0.227	0.225
n [F mol^{-1}]		1.99	2.06	2.05	1.96

The transfer coefficient (α) is defined as the rate of change of the free energy of activation as a function of the free energy of ET, namely $(d\Delta G^\ddagger / d\Delta G_{\text{ET}}^\circ)$. It can be calculated from the experimental data from either the variation of E_p with ν through the slope of a plot of $\log \nu$ against E_p or from $\Delta E_{p/2}$ data.^[56, 71] For **ASC** and **DASC**, α decreases with increasing scan rate over the potential scan rates investigated (Table 1), and average values of $\alpha = 0.24$ are found in both MeCN and DMF. The low α and its scan rate dependence indicate that the heterogeneous rate constant, k_{het} , for ET from electrode to **ASC** and **DASC** is rate determining. The voltammetric

behavior further indicates that the ET reduction of these endoperoxides is governed by the kinetics of the ET process and, thus, cannot be described by Butler–Volmer kinetics. Since the ET is rate determining, the observed E_p is more negative than the thermodynamic standard potential (E_{diss}°). The determination of the E_{diss}° is one of the key aspects of the present study, and will be discussed below.

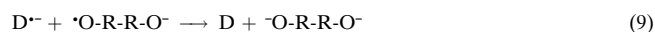
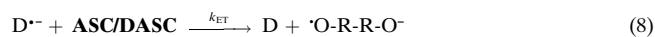
Preparative electrochemical studies were also done, and the coulometric results of the electrolyses of **ASC** and **DASC** on a carbon electrode are summarized in Table 1. Electrolysis leads to the consumption of approximately 2 F mol^{-1} , or two electron equivalents, in both solvents in the presence and absence of acid. Work-up and isolation after electrolysis yield quantitatively the corresponding *cis*-diols, namely *cis*-1-isopropyl-4-methylcyclohexane-1,4-diol and *cis*-1-isopropyl-4-methylcyclohex-2-ene-1,4-diol, in both solvents. The results of the voltammetric and product studies are consistent with the dissociative reduction of the O–O bond by the overall two-step, two-electron process illustrated for **ASC** in Equations (5) and (6).



According to this mechanism, the first electron results in a concerted dissociative fragmentation affording $\cdot\text{O-R-R-O}^-$, a species that we term the distonic radical anion. Formation of a similar intermediate on reduction of **ASC** in the presence of Fe(II) was proposed previously.^[72] In this study, the resulting radical reacted to give high yields of β -scission products. Such competing radical processes do not occur in our system under the electrochemical conditions. At the potential where $\cdot\text{O-R-R-O}^-$ is generated (or $\cdot\text{O-R-R-OH}$), its reduction to the dialkoxide (or $^- \text{O-R-R-OH}$) is strongly favored, by using the reasonable assumption that the reduction potential of the distonic radical anion is similar to that of the *tert*-butyl alkoxy radical ($E^\circ = -0.30 \text{ V}$ vs. SCE in MeCN and -0.23 V vs. SCE in DMF).^[47, 48] In principle, even if intermediate alkoxy radicals abstract hydrogen atoms from solvent, particularly DMF, there are no complications to our analysis described below, since the resulting solvent radical will be at a potential where reduction is also a driven process.^[45] The net result is still a two electron reduction, in which the first ET is rate determining.

Homogeneous electron-transfer reduction: The reduction of **ASC** and **DASC** by homogeneous electron-transfer techniques was studied. In these experiments an extensive series of electro-generated donor radical anions ($\text{D}^{\bullet-}$) were used as the electron source, and react according to Equations (7)–(9). Part of this work was reported briefly in our preliminary communication and involved using both the method of homogeneous redox catalysis^[73–75] and, for measurement of

some of the slower reactions, the method outlined by Pedersen and Daasbjerg.^[76, 77] In the former, the catalytic increase in current for the reduction of the donor, measured as a function of varying concentrations of **ASC** or **DASC** at different scan rates, was compared with data obtained by simulation of the two electron mechanism outlined in Equations (8) and (9) to obtain k_{ET} .



In none of the cases was there evidence for any competing reactions between the donor and endoperoxides or between the donor radical anion and distonic radical anion. The involvement of reactions of the mediator radical anion with endoperoxide (or with solvent) was tested by monitoring the extent of recovery of mediator after electrolysis of 2 F mol^{-1} with one half equivalent of the endoperoxide. At least 98% of the mediator was recovered, even in the cases for slow dissociative ET, where competing reactions of the radical anion with electrophilic impurities could occur.

Kinetic data obtained from an average of at least three independent experiments in both MeCN and DMF are summarized in Table 2. Data corresponding to the slowest reactions that define the parabolic shape of a plot of $\ln(k_{\text{hom}})$ against the E° of the donors have been performed more often and with a variety of donors with similar E° to verify the value of the rate constants with donors at that potential. In general, the reaction rate constants increase as the standard potential of the mediator becomes more negative (this corresponds to an increase in driving force for reaction Equation (8)). The kinetic data are independent of the solvent system (DMF or MeCN).

The homogeneous ET kinetic data can be related to the transfer coefficient, α , through $\alpha = -(RT/F)d(\ln k_{\text{ET}})/dE$. Thus, taking the derivative of the quadratic fit of the combined $\ln(k_{\text{hom}})$ versus E° data gives equations α

$= 1.55 + 0.808 E$ and $\alpha = 1.22 + 0.561 E$ for **ASC** and **DASC**, respectively. An α value of 0.5 corresponds to the dissociative reduction potentials, E_{diss}° , for **ASC** and **DASC** and gives values of -1.30 V and -1.28 V , respectively. These values show that the observed E_p values of the heterogeneous reduction overestimate the true standard potential by at least 0.6 V .

Heterogeneous ET reduction: The kinetics of ET to **ASC** and **DASC** were studied by heterogeneous reduction, in which the electron source in Equation (5) was a glassy carbon electrode. A convolution analysis approach was used to study the heterogeneous electron-transfer kinetics of the dissociative reduction of **ASC** and **DASC**. This method, for which the experimental and theoretical treatments have been described in detail previously,^[46, 59, 78, 79] has only recently proven to be powerful for the determination of the standard potentials for systems that undergo dissociative ET. In particular, it has been successfully used to study the direct reduction of a number of acyclic dialkyl peroxides^[46, 48] and perbenzoates.^[78, 80] We have used this method to determine the standard reduction potential of the antimalarial trioxane, Artemisinin.^[49]

The collection of high-quality cyclic voltammograms is essential for meaningful thermochemical information to be extracted from the acquired data. A sample of background-subtracted linear-scan voltammograms measured between 0.1 V s^{-1} and 10 V s^{-1} for **ASC** is shown in Figure 2a. Convolution of the voltammetric curves yields limiting current values, I_{lim} , that are independent of scan rate. The voltammetric curves correspond to the uptake of two electrons per molecule; this is consistent with the two-step fragmentation mechanism in Equations (5) and (6). I is related to the actual current i through the convolution integral.^[71, 81] The I against E plot is a wave-like curve and the plateau value is reached when the applied potential is sufficiently negative. The result of this analysis for **ASC** is shown in Figure 2b. Under these conditions (diffusion control), I reaches its limiting value, I_{lim} , defined as $I_{\text{lim}} = nFAD^{1/2}C^*$, where n is the overall electron consumption, A

Table 2. Rate constants for electron transfer ($\log k_{\text{ET}}$) from electrochemically generated donors ($\text{D}^{\cdot-}$) with varying standard potentials (E°) to **ASC** and **DASC** in 0.1M TEAP/DMF and MeCN solutions at 25°C .

Donor	E° (MeCN) versus SCE ^[a]	E° (DMF) versus SCE ^[a]	ASC		DASC	
			$\log k_{\text{ET}}^{\text{[b]}}$ MeCN	$\log k_{\text{ET}}^{\text{[b]}}$ DMF	$\log k_{\text{ET}}^{\text{[b]}}$ MeCN	$\log k_{\text{ET}}^{\text{[b]}}$ DMF
perylene	-1.674	-1.640	4.00	3.86	4.06	3.78
acenaphthylene	-1.651	-1.629	3.64	3.42	3.43	3.45
1,4-dicyanobenzene	-1.576	[d]	3.44	[d]	3.20	[d]
tetracene	[e]	-1.548	[d]	3.43	[d]	3.20
4,4'-dimethoxyazobenzene	-1.526	-1.531	2.91	3.08	2.75	2.78
4-methyl-4'-methoxyazobenzene	-1.478	-1.478	2.75	2.97	2.51	2.49
4-methoxyazobenzene	-1.426	-1.424	2.47	2.60	2.05	2.17
azobenzene	-1.335	-1.316	1.75	1.94	1.81	1.47
3,3'-dimethoxyazobenzene	-1.278	-1.258	1.39	1.62	1.42	1.32
2-nitrobiphenyl	-1.157	-1.186	0.157	0.822	0.240	0.204
nitrobenzene	-1.100	-1.100	-0.477 ^[e]	-0.767 ^[e]	-0.647 ^[e]	-1.030 ^[e]
4-nitrobiphenyl	[d]	-1.078	[d]	[d]	[d]	-0.976 ^[e]
1-nitronaphthalene	-1.041	-1.040	-0.602 ^[e]	-1.230 ^[e]	[d]	-0.899 ^[e]

[a] E° measured versus an internal standard (ferrocene) and corrected: $\text{Fc}/\text{Fc}^+ = 0.449 \text{ V}$ against SCE in MeCN and 0.475 V against SCE in DMF. [b] Measured by homogeneous redox catalysis (ref. [73–75]). [c] Not soluble. [d] Not measured. [e] Measured by using methods outlined in refs. [76] and [77].

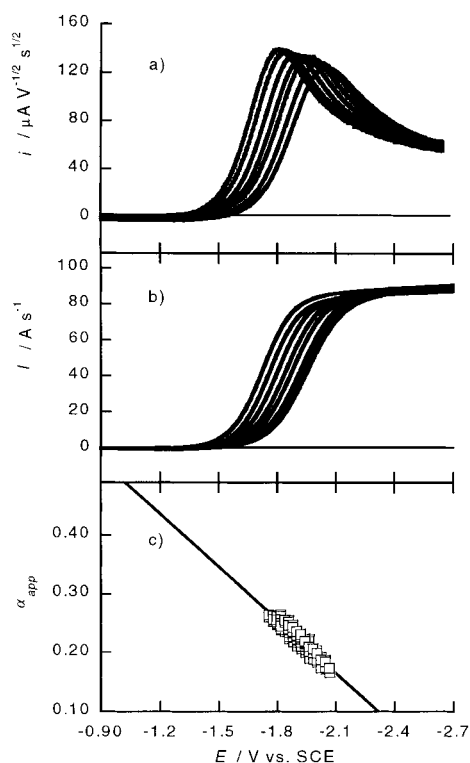


Figure 2. a) Background-subtracted linear-scan voltammograms for 2 mmol L⁻¹ ASC in ACN with 0.1 mol L⁻¹ TEAP and excess 2,2,2-trifluoroethanol at a glassy carbon electrode. The voltammetric data is in its ν -normalized form. The scan rates were 0.1, 0.5, 1, 2, 5, and 10 V s⁻¹. b) Corresponding convolution curves at scan rates 0.1, 0.2, 0.5, 1, 2, 5, 8, and 10 V s⁻¹. c) Potential dependence of the apparent transfer coefficient for the reduction.

the electrode area, D the diffusion coefficient, and C^* the substrate concentration. Since I is related to the surface concentration of reactant and product, an equation relating k_{het} to i and I can be derived. For a totally irreversible process, as is the case for the reduction of ASC and DASC, at constant I_{lim} the limiting current can be related to k_{het} by using the expression:

$$\ln k_{\text{het}} = \ln D^{1/2} - \ln \left(\frac{[I_{\text{lim}} - I(t)]}{i(t)} \right)$$

For ASC and DASC the diffusion coefficients were determined to be $2.36 \times 10^{-5} \text{ cm}^2 \text{ s}^{-1}$ in MeCN and $1.08 \times 10^{-5} \text{ cm}^2 \text{ s}^{-1}$ in DMF, respectively, by using the Taylor dispersion method.^[82, 83] When corrected for the viscosity change of solvent with 0.1 M TEAP according to the Stokes–Einstein relation, the D values become $2.16 \times 10^{-5} \text{ cm}^2 \text{ s}^{-1}$ and $9.93 \times 10^{-6} \text{ cm}^2 \text{ s}^{-1}$, respectively. Convolution analysis of 20 sets of data measured at 1 mV intervals provide $\ln k_{\text{het}}$ data that can be plotted against the driving force, E . By using the usual activation–driving force relationship $\ln k_{\text{het}}$ versus E data is related to the apparent transfer coefficient α_{app} . Each curve from the $\ln k_{\text{het}}$ data is fitted to the above equation in 21 mV segments. The result of this analysis for ASC is shown in Figure 2c; similar results were determined for DASC and are not shown. Alpha values determined in this way agree with those summarized in Table 1. In principle, these values can be used similarly to the homogeneous data to obtain estimates of

the standard dissociative reduction potential of ASC and DASC. Doing this yields E_{diss}° values of -1.0 and -0.97 V, respectively. These values are 0.3 V less negative than those estimated by the homogeneous approach.

It is interesting to compare the homogeneous and heterogeneous approaches. In the former, the amount of measurable data is small and limited to the number and range of donors that can be used. In the latter, the free energy of the reaction is varied continuously and, thus, the amount of data in a particular free energy range is large, although the range of free energy over which data can be measured is limited by the scan rates that can be investigated. While we somewhat prefer the E_{diss}° values obtained by homogeneous data, because of the limited potential range over which the heterogeneous data could be measured, the E_{diss}° values we use below in $\Delta G_{\text{ET}}^{\circ}$ calculations are the average values from the two approaches to better reflect the uncertainty in the estimate; thus, $E_{\text{diss}}^{\circ} = -1.2 \pm 0.2$ and -1.1 ± 0.2 V for ASC and DASC, respectively. It must be stressed that these average E_{diss}° values provide a more accurate determination of the standard reduction potential than those estimated from the peak potential.

Both the heterogeneous and homogeneous ET rate-constant data can thus be plotted against the free energy of ET, by taking into account that $\Delta G_{\text{ET}}^{\circ} = F(E_{\text{D/D}^{\cdot-}}^{\circ} - E_{\text{diss}}^{\circ})$ and using the average E_{diss}° values for ASC and DASC; these plots are shown in Figure 3a and b for ASC and DASC, respectively. The homogeneous kinetic data from Table 2 shows the fit to Equations (2)–(4) as described below.

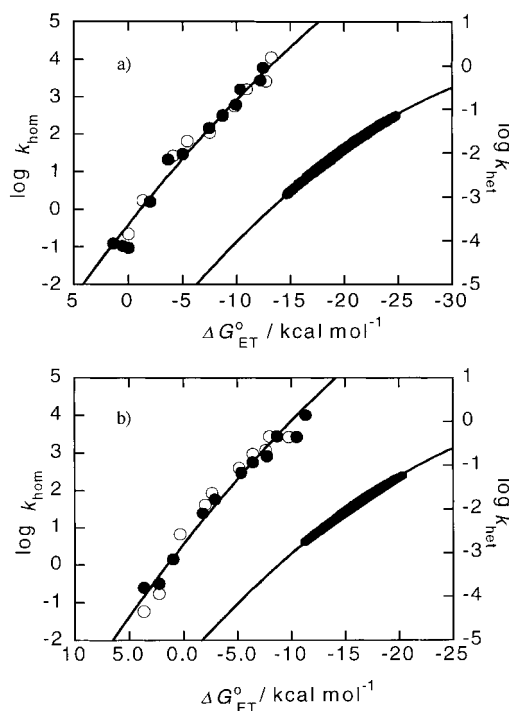


Figure 3. Composite plot of $\log k_{\text{hom}} [\text{M}^{-1} \text{ s}^{-1}]$ versus $\Delta G_{\text{ET}}^{\circ}$ (left) with plots of $\log k_{\text{het}} [\text{cm}^2 \text{ s}^{-1}]$ versus $\Delta G_{\text{ET}}^{\circ}$ (right) for a) DASC and b) ASC. The heterogeneous plot is a composite of 25 separate experiments where the scan rate was varied between 0.1 and 10 V s⁻¹. The solid line through the homogeneous data is fitted according to Equations (2) and (4) with the parameters summarized in the text and by using the nonadiabatic Z term. The solid line through the heterogeneous data is to a simple second-order polynomial.

Temperature dependence of the rate constants: Activation parameters for the reduction of **ASC** and **DASC** were measured from a temperature study by using a pair of donors, acenaphthylene and 4,4'-dimethoxyazobenzene. These studies provided $\log A$ values of 7.1–7.5 and E_a values of 4.9–6.0 kcal mol⁻¹ for **ASC** and $\log A$ values of 7.6–7.8 and E_a values of 5.7–6.8 kcal mol⁻¹ for **DASC**. (See Supporting Information for complete details.) Interestingly, the pre-exponential factors are 2.5–3 orders of magnitude lower than those calculated for an adiabatic ET process by the methods previously described.^[48] Therefore, the adiabatic dissociative ET model does not account for the experimental kinetic data for these endoperoxides. The unusually low, measured pre-exponential factors are, however, predicted by the theory for nonadiabatic dissociative ET^[84] and consistent with our recent results for ET to acyclic peroxides, which is nonadiabatic due to poor electronic coupling between the reactant and product electron potential energy surfaces.^[48]

Determination of thermochemical parameters: Savéant's theory of dissociative ET can be applied to the $\log k_{\text{ET}}$ versus $\Delta G_{\text{ET}}^\circ$ data for **ASC** and **DASC** [Eqs. (2)–(4)] to determine valuable thermochemical information, such as the intrinsic barrier ΔG_0^\ddagger .^[56, 57, 60, 61] The kinetic plots shown in Figure 3 are constructed from the homogeneous data summarized in Table 2, the heterogeneous kinetic data obtained by convolution analysis and our subsequent determination of E_{diss}° . These figures convincingly illustrate the parabolic nature of and provides support for the activation–driving force relationship described by Equations (2)–(4). The amount of curvature in the data depends on ΔG_0^\ddagger , which itself depends on the reorganization energy and BDE for the dissociative reduction. Both sets of data can be fitted according to Equations (2)–(4) to provide an estimate for ΔG_0^\ddagger by using an estimate of the nonadiabatic pre-exponential factor ($\kappa_{\text{el}}Z$).

An estimate of $\kappa_{\text{el}}Z$ for the present work was determined by using the homogeneous ET kinetics of di-*tert*-butylperoxide determined from the previous study.^[47, 48] Using a value of $\Delta G_0^\ddagger = 13.1$ kcal mol⁻¹ leads to a value of $4.3 \times 10^8 \text{ M}^{-1} \text{ s}^{-1}$ for the $\kappa_{\text{el}}Z$ for di-*tert*-butylperoxide. To give an estimated $\kappa_{\text{el}}Z$ for the nonsterically encumbered **ASC/DASC** in this study, we added a further correction of 0.8 log units to remove the contribution of the steric effect imposed by the bulky *tert*-butyl groups of di-*tert*-butylperoxide. This latter value was estimated by comparison of the difference in k_{het} values between di-*tert*-butylperoxide and di-*n*-butylperoxide at similar driving forces; these two endoperoxides have the same BDE.^[48] This leads to an estimated $\kappa_{\text{el}}Z$ of $2.7 \times 10^9 \text{ M}^{-1} \text{ s}^{-1}$. The $\log k_{\text{hom}}$ versus $\Delta G_{\text{ET}}^\circ$ data for **ASC** and **DASC** were then fitted to Equations (2)–(4) by using this $\kappa_{\text{el}}Z$ value to determine the intrinsic barriers, ΔG_0^\ddagger . The fits are shown in Figure 3 as solid lines through the data and provide values for ΔG_0^\ddagger of 11.9 and 9.6 kcal mol⁻¹ for **ASC** and 13.2 and 11.0 kcal mol⁻¹ for **DASC** from the homogeneous and heterogeneous data, respectively.

Values for ΔG_0^\ddagger can be related to the BDE and the solvation energy (λ) since $\Delta G_0^\ddagger = (\lambda + \text{BDE})/4$. We assume that the BDE for **ASC** and **DASC** is the same within error.

Values for the BDE of **ASC** and **DASC** can be estimated from gas-phase bond-dissociation enthalpy for the homolytic cleavage of 1,4-dimethyl-2,3-dioxabicyclo[2.2.2] octane. The heat of formation of the endoperoxide was estimated to be -50.53 kcal mol⁻¹ from ab initio energies, following a group contribution procedure analogous to that of Schleyer and Ibrahim, with the following changes: energies were calculated at the B3LYP/6–31G**//RHF/6–31G** level and groups were defined by Benson. The heat of formation of the $\cdot\text{O-R-R-O}\cdot$ diradical was estimated to be -21.4 kcal mol⁻¹. Using these values provides O–O BDE of 29 kcal mol⁻¹. The BDE for **ASC** is significantly lower than the value 37 kcal mol⁻¹ for the BDE of acyclic peroxides.^[48] This difference is expected based on the added molecular strain and repulsive forces due to the eclipsing interactions of the lone pairs on the oxygen atoms in **ASC** and **DASC**.

Interestingly, this value of the BDE is the same as that estimated from an expression derived by Savéant that relates the BDE to the E_p of the dissociative process and the oxidation potential of the anion fragment, namely $E_{\text{RO}\cdot/\text{RO}^-}^\circ$. If one makes the assumption that $E_{\text{HORRO}\cdot/\text{HORRO}^-}^\circ$ is equal to the standard potential of the tertiary alkoxy radical $E_{i\text{BuO}\cdot/i\text{BuO}^-}^\circ$, then the ΔBDE between di-*tert*-butylperoxide and **ASC** can be estimated from $\Delta\text{BDE} = -2/3[E_p(\text{di-}i\text{tert-butyl peroxide}) - E_p(\text{ASC})]$. Since the BDE of the O–O bond in di-*tert*-butyl peroxide is 37 kcal mol⁻¹ and its $E_p = -2.50$ under the same conditions, the BDE of **ASC** is estimated to be 28 kcal mol⁻¹. It should be stressed that this latter relationship of Savéant's is uncertain, and the fact that our theoretical estimation is the same may be fortuitous.

By using the above estimate for BDE and the ΔG_0^\ddagger obtained from the fit of the data, the homogeneous reorganization energies (λ^{hom}) were determined to be 19.4 and 24.3 kcal mol⁻¹ for **ASC** and **DASC**, respectively. It should be noted that λ^{hom} values obtained from the fits by using the usual adiabatic Z term ($3 \times 10^{11} \text{ s}^{-1}$) are 9–12 kcal mol⁻¹ higher and do not agree with estimates below. Estimates for the homogeneous solvation energy can also be obtained by using expressions by Marcus and Kojima–Bard^[48, 85] and a similar expression with a modified term suggested by Savéant.^[56] Accurate values for radius of the donor, r_D , and the radius of the acceptor, r_{AB} , are required for a reasonable estimate of λ^{hom} ; these were estimated from the following procedure. The radius of **ASC** was determined from the density of the compound by using $r(\text{\AA}) = 10^8[(3M/4\pi N_A\rho)^{1/3}]$ and from the diffusion coefficient calculated by the Stokes–Einstein equation. It is expected that most of the charge in the distonic radical anion is localized on the oxygen atom and that it is shielded from the rest of the molecule. Thus we use an effective radius that better accounts for this smaller area where the charge is localized. The effective radii, r_{eff} , was determined by using $r_{\text{eff}} = [r_A(2r_{\text{AB}} - r_A)/r_{\text{AB}}]$, where AB refers the starting endoperoxide and A the *tert*-butyl alkoxide anion, similar to the anion that is generated in the ET.^[48, 56] An effective radius for the *tert*-butyl alkoxide anion was determined similarly with AB as the radius of *tert*-butyl alkoxide and B the radius of an oxygen atom.^[46] It was assumed that **ASC** and **DASC** have the same radius. An average r_D of 3.80 Å was chosen for the donors. The calculated effective

radii is 2.76 Å. This radius leads to a λ^{hom} of 15.2 kcal mol⁻¹ by using the Kojima–Bard approach and 15.9 kcal mol⁻¹ with Savéant's approach.

The slope of the regression analysis of the α versus E plots is directly linked to the intrinsic barrier through the expression $da/dE = F/8\Delta G_0^\ddagger$. With the BDE for **ASC** and **DASC** known, the heterogeneous solvation energy, λ^{het} is 9.9 kcal mol⁻¹ for **ASC** and 15.5 kcal mol⁻¹ for **DASC**. These can be compared with calculated values by using the approaches of Marcus (13.9 kcal mol⁻¹) and Kojima–Bard (20.2 kcal mol⁻¹)^[85].

The values obtained for ΔG_0^\ddagger and λ from the homogeneous and heterogeneous data are comparable to previously reported values obtained for other O–O systems, including the trioxane, artemisinin, and a number of acyclic peroxides.^[46, 48, 49] In general, the intrinsic free energies are similar for all systems, within error (an error of 0.1 V in E_{diss}° manifests itself as an error of 1 kcal mol⁻¹ in ΔG_0^\ddagger). Since the BDE of the endoperoxides is much lower than that of the acyclic peroxides, the result is a somewhat higher average value for λ . Keeping in mind that an error of 1 kcal mol⁻¹ in ΔG_0^\ddagger leads to more uncertainty in λ , it is tempting to think that the higher λ values in the endoperoxides may reflect additional internal reorganization energy in these strained systems. Such contributions are generally considered to be small in dissociative processes with large BDEs but, with the much lower BDEs in these endoperoxides, they may contribute to the intrinsic barrier. Also of interest is the observation that the λ is larger for **DASC** than **ASC**. **DASC**, lacking the alkene moiety, is somewhat more floppy than **ASC**. This floppiness is reflected in the C–O–O–C dihedral angles (0° in **ASC** against 15° in **DASC**).^[86]

Conclusion

ASC and **DASC** undergo a concerted dissociative reduction by an ET to the σ^* orbital of the O–O bond. The systems reported here provide interesting cases for testing the theories of dissociative ET since, on reduction, both the charged and the radical fragments remain in the same molecule. We provide the only reliable and most comprehensive kinetic data to date for ET to these types of cyclic O–O systems and use them to determine accurate standard reduction potentials for model endoperoxides. Further, our temperature-dependent rate studies provide support for the theory that the concerted dissociative ET to endoperoxides is nonadiabatic. Like the O–O bond in acyclic peroxides, the nonadiabaticity and thus poor electronic coupling between reactant and product surfaces may be the result of the symmetry of the O–O bond and the lack of change in dipole moment during bond stretching in the transition state. In addition to providing the best example of the quadratic nature of the activation–driving relationship for dissociative ETs, fits of the homogeneous and heterogeneous ET kinetic data to nonadiabatic ET theory provide an estimate of ΔG_0^\ddagger . The use of a reasonable BDE for this system provides an understanding of the reorganization energies. Now that the thermochemical properties of O–O reduction are better understood, the electrochemical approaches described herein may be used to

determine BDE and other thermochemical parameters for other endoperoxides, especially those of biological relevance.

Experimental Section

Materials: Ascaridole and dihydroascaridole were synthesized by standard literature procedures^[87, 88] and purified by distillation with a Kugelrohr apparatus at 40 °C (0.025 mm). CAUTION: Peroxides are potentially explosive; heat with care. The homogeneous ET mediators 9,10-diphenylanthracene, fluoranthene, perylene, acenaphthylene, 1,4-dicyanobenzene, tetracene, azobenzene, 2-nitrobiphenyl, nitrobenzene, 4-nitrobiphenyl, and 1-nitronaphthalene were used as received from Aldrich. Other mediators were synthesized: 4-methoxyazobenzene (m.p. 55–56 °C) and 4-methoxy-4-methylazobenzene (m.p. 100–100.5 °C) were made by treatment of the corresponding hydroxy-substituted azobenzenes with methyl iodide and potassium carbonate in acetone. 4,4'-dimethoxyazobenzene,^[89] 3,3'-dimethoxyazobenzene^[90] and 4-hydroxy-4'-methylazobenzene^[91] were made by following literature procedures. All of the substituted azobenzenes were recrystallized with an appropriate solvent or purified by column chromatography according to the corresponding literature procedure before use. Spectroscopic grade *N,N*-dimethylformamide (Lancaster) was distilled over CaH₂ under nitrogen at reduced pressure. Spectroscopic grade acetonitrile (BDH) was distilled over CaH₂ and run through a column of activated alumina prior to storage. Both solvents were stored over alumina, which had been activated at 350 °C while under vacuum (0.02 mm Hg), for 48 hours. Tetraethylammonium perchlorate (TEAP, Aldrich) was recrystallized three times from ethanol and dried under vacuum at 60 °C.

Nuclear magnetic resonance spectra were recorded on a Varian XL300 spectrometer with tetramethylsilane as the internal reference standard. IR spectra were recorded on Aviv-17 IR spectrometer and mass spectra were recorded on a MAT8200 Finigan high resolution mass spectrometer.

Electrochemical apparatus and procedures: Cyclic voltammetry was performed by using a PAR283 or 263 potentiostat interfaced to a personal computer with PAR270 electrochemistry software. A three-electrode arrangement was used in the electrochemical cell.^[71] The cell ohmic drop was compensated for by using a positive feedback approach and adjusted to at least 98 % of the oscillation value. The electrodes and a stir-bar were assembled in a water-jacketed electrochemical cell, while in an oven at 100 °C, and placed in a Faraday cage to cool under a continuous flow of high-purity dry argon. An argon atmosphere was maintained throughout the experiment to protect the contents of the cell from atmospheric oxygen and moisture. After cooling, a temperature of 25 °C was maintained through the jacketed cell by using a circulating water bath. For the temperature-dependence studies, the temperature was controlled by a VWR Scientific Model 1150A constant-temperature circulator; the cell was allowed to equilibrate for 30 minutes at each temperature. The appropriate solvent and 0.1M electrolyte were added to the cell, and oxygen was purged from the solution with argon. Throughout the experiment, an argon atmosphere was maintained. The working electrode was a 3 mm diameter glassy carbon rod (Tokai, GC-20) sealed in glass tubing. Prior to each experiment, the working electrode was freshly polished with 0.25 μm diamond paste and ultrasonically rinsed in 2-propanol for fifteen minutes. Electrochemical activation of the electrode was carried out in the background solution by cycling several times between 0 and –2.7 V versus SCE at a 0.2 V s⁻¹ scan rate. The surface area was calculated with reference to the diffusion coefficient of ferrocene in ACN and DMF with TEAP (0.1M). The counter electrode was a platinum plate placed symmetrically under the working electrode. The reference electrode was made of a silver wire immersed in a glass tube with a fine sintered bottom containing TEAP (0.1M) in the desired solvent. Its potential remained constant for the duration of the experiment and was then calibrated by adding ferrocene. In these studies, the standard potential of the ferrocene/ferrocenium couple was 0.449 V and 0.475 V versus SCE for ACN and DMF, respectively. All reported potentials are referenced to SCE.

Standard potentials for the homogeneous donors were determined in a standard voltammetry cell. Cyclic voltammograms at scan rates ranging from 0.1 to 5 V s⁻¹ of a 1–3 mmol L⁻¹ solution of donor were obtained, then

ferrocene was added to the cell and a series of ferrocene/ferrocenium voltammograms were acquired. The standard potentials for the reversible homogeneous donors and ferrocene were determined as the average of the anodic and cathodic peak potentials. Simulation of homogeneous redox catalysis data was performed with Digisim 2.1® software.

Preparative electrolysis: All preparative electrolysis was carried out in argon-purged solutions containing TEAP (0.1M, 25 mL), with the reference and glassy carbon electrode described for cyclic voltammetry. The working electrode was a reticulated vitreous-carbon or platinum gauze and the anode a platinum wire that was separated by a glass tube with a sintered bottom and a 3 mm layer of neutral alumina. Constant potential electrolysis was carried out in an identical cell to that described for constant current electrolysis, except that the electrodes were connected to a potentiostat. Electrolysis was carried out at a potential of approximately 100 mV past the peak maximum and continued until the current was reduced to the initial background level.

A cyclic voltammogram on a small 3 mm glassy carbon electrode was used as a probe for the concentration of the substrate in the electrolysis cell in both constant potential and constant current experiments. After electrolysis, water (40 mL) was added to the cell, and the contents were extracted with dichloromethane (4 × 20 mL). The organic extracts were then washed with water (2 × 20 mL), dried over sodium sulfate, filtered and evaporated.

In the preparative scale electrolysis of **ASC** and **DASC**, only one product was formed in each; this corresponded to the following: electrolysis of **ASC**: *cis*-1-isopropyl-4-methylcyclohex-2-ene-1,4-diol. ¹H NMR (CDCl₃): δ = 0.87 (d, *J* = 6.9 Hz, 3H), 0.93 (d, *J* = 6.9 Hz, 3H), 1.23 (s, 3H), 1.62–1.87 (m, 7H), 5.53 (dd, *J* = 10.1, 1.3 Hz, 1H), 5.69 (dd, *J* = 10.1, 1.3 Hz, 1H); ¹³C NMR (CDCl₃): δ = 16.72, 18.74, 27.38, 35.19, 37.52, 69.88, 72.18, 137.54, 132.36; IR: 3353 cm⁻¹ (br), 3024, 2969, 2880, 1606, 1374, 1381, 1138, 1004; MS: *m/z* (%): 155 (12), 127 (62), 109 (100). Deuterium exchange verified that there were two alcoholic protons.

Electrolysis of **DASC**: *cis*-1-isopropyl-4-methylcyclohexane-1,4-diol. ¹H NMR (CDCl₃): δ = 0.85 (d, *J* = 6.9 Hz, 6H), 1.15 (s, 3H), 1.32–1.86 (m, 10H); ¹³C NMR (CDCl₃): δ = 16.76, 25.79, 31.89, 35.78, 36.11, 38.76, 70.25; MS: *m/z* (%): 154 (8), 139 (10), 129 (15), 111 (100); IR: 3353 cm⁻¹ (br), 2956, 2875, 1371, 1379, 1123, 998. Deuterium exchange verified that there were two alcoholic protons.

Acknowledgements

The financial support of the Natural Sciences and Engineering Research Council of Canada (NSERC), the Canadian Foundation for Innovation, ORCDF, and the University of Western Ontario (ADF) is gratefully acknowledged. R.L.D. thanks NSERC for a PGS scholarship. Professor Flavio Maran is thanked graciously for numerous and fruitful discussions, and for providing analysis software.

- [1] E. L. Clennan, C. S. Foote in *Organic Peroxides* (Ed.: W. Ando), Wiley, Chichester, England, **1992**, p. 225.
- [2] D. A. Casteel, *Nat. Prod. Rep.* **1999**, *16*, 55.
- [3] R. G. Salomon, *Acc. Chem. Res.* **1985**, *18*, 294.
- [4] W.-S. Zhou, X.-X. Xu, *Acc. Chem. Res.* **1994**, *27*, 211.
- [5] J. A. Vroman, I. A. Khan, M. A. Avery, *Tetrahedron Lett.* **1997**, *38*, 6173.
- [6] G. H. Posner, L. González, J. N. Cumming, D. Klinedinst, T. A. Shapiro, *Tetrahedron* **1997**, *53*, 37.
- [7] F. Zouhirri, D. Desmaële, J. d'Angelo, J. Mahuteau, C. Riche, F. Gay, L. Ciceron, *Eur. J. Org. Chem.* **1998**, 2897.
- [8] E. Van Geldre, A. Vergauwe, E. Van den Eeckhout, *Plant Mol. Biol.* **1997**, *33*, 199.
- [9] G. H. Posner, H. O'Dowd, T. Caferro, J. N. Cumming, P. Ploypradith, S. Xie, T. A. Shapiro, *Tetrahedron Lett.* **1998**, *39*, 2273.
- [10] H. O'Dowd, P. Ploypradith, S. Xie, T. A. Shapiro, G. H. Posner, *Tetrahedron* **1999**, 55.
- [11] S. R. Meshnick, T. E. Taylor, S. Kamchonwongpaisan, *Microbiol. Rev.* **1996**, *60*, 301.
- [12] M. Jung, S. Lee, *Heterocycles* **1997**, *45*, 1055.
- [13] C. W. Jefford, M. G. H. Vicente, Y. Jacquier, F. Favarger, J. Mareda, P. Millasson-Schmidt, G. Brunner, U. Burger, *Helv. Chim. Acta* **1996**, *79*, 1475.
- [14] R. K. Haynes, S. C. Vonwiller, *Acc. Chem. Res.* **1997**, *30*, 73.
- [15] M. Hamzaoui, O. Provot, B. Camuzat-Dedenis, H. Moskiwitz, J. Mayrargue, L. Cicéron, F. Gay, *Tet. Lett.* **1998**, *39*, 4029.
- [16] J. N. Cumming, D. Wang, S. B. Park, T. A. Shapiro, G. H. Posner, *J. Med. Chem.* **1998**, *41*, 952.
- [17] G. H. Posner, M. H. Parker, J. Northrop, F. S. Elias, P. Ploypradith, S. Xie, T. A. Shapiro, *J. Med. Chem.* **1999**, *42*, 300.
- [18] G. H. Posner, J. N. Cumming, S.-H. Woo, P. Ploypradith, S. Xie, T. A. Shapiro, *J. Med. Chem.* **1998**, *41*, 940.
- [19] J. Bhisutthibhan, X.-C. Pan, D. J. Hossler, D. J. Walker, C. A. Yowell, J. Carlton, J. B. Dame, S. R. Meshnick, *J. Biol. Chem.* **1998**, *273*, 16192.
- [20] Y. Wu, Y. Y. Zheng, Y.-L. Wu, *Angew. Chem.* **1999**, *111*, 2730–2733; *Angew. Chem. Int. Ed.* **1999**, *38*, 2580.
- [21] W.-M. Wu, Y. Wu, Y.-L. Wu, Z.-J. Tao, C.-M. Zhou, Y. Li, F. Shan, *J. Am. Chem. Soc.* **1998**, *120*, 3316.
- [22] A. Robert, B. Meunier, *Chem. Eur. J.* **1998**, *4*, 1287.
- [23] G. H. Posner, D. Wang, L. González, X. Tao, J. N. Cumming, D. Klinedinst, T. A. Shapiro, *Tetrahedron Lett.* **1996**, *37*, 815.
- [24] A. Robert, B. Meunier, *Chem. Soc. Rev.* **1998**, *27*, 273.
- [25] R. K. Haynes, S. C. Vonwiller, *Tetrahedron Lett.* **1996**, *37*, 253.
- [26] R. K. Haynes, S. C. Vonwiller, *Tetrahedron Lett.* **1996**, *37*, 257.
- [27] A. Robert, G. Meunier, *J. Am. Chem. Soc.* **1997**, *119*, 5968.
- [28] G. H. Posner, S. B. Park, L. González, D. Wang, J. N. Cumming, D. Klinedinst, T. A. Shapiro, M. D. Bachi, *J. Am. Chem. Soc.* **1996**, *118*, 3537.
- [29] P. M. O'Neill, L. P. Bishop, N. J. Searle, J. L. Maggs, S. A. Ward, P. G. Bray, R. C. Storr, B. K. Park, *Tetrahedron Lett.* **1997**, *38*, 4263.
- [30] W. Adam, A. Schonberger, *Chem. Ber.* **1992**, *125*, 2149.
- [31] J. Koo, G. B. Schuster, *J. Am. Chem. Soc.* **1978**, *100*, 4496.
- [32] G. B. Schuster, *Acc. Chem. Res.* **1979**, *12*, 366.
- [33] G. B. Schuster in *Advances in Electron Transfer Chemistry Vol. 1* (Ed.: P. S. Mariano), JAI Press, Greenwich, **1991**, p. 163.
- [34] J. J. Zupancic, K. A. Horn, G. B. Schuster, *J. Am. Chem. Soc.* **1980**, *102*, 5279.
- [35] W. Adam, I. Erden, *Angew. Chem.* **1978**, *90*, 223; *Angew. Chem. Int. Ed. Engl.* **1978**, *17*, 210.
- [36] W. Adam, O. Cueto, *J. Am. Chem. Soc.* **1979**, *101*, 6511.
- [37] W. Adam, K. Zinner, A. Krebs, H. Schmalstieg, *Tetrahedron Lett.* **1981**, *22*, 4567.
- [38] Y. Takano, T. Tsunesad, H. Isobe, Y. Yoshioka, K. Yamaguchi, I. Saito, *Bull. Chem. Soc. Jpn.* **1999**, *72*, 213.
- [39] T. Wilson, *Photochem. Photobiol.* **1995**, *62*, 601.
- [40] W. Adam, A. V. Trofimov, *J. Org. Chem.* **2000**, *65*, 6474.
- [41] W. Adam, M. Matsumoto, A. V. Trofimov, *J. Org. Chem.* **2000**, *65*, 2078.
- [42] W. Adam, M. Matsumoto, A. V. Trofimov, *J. Am. Chem. Soc.* **2000**, *122*, 8631.
- [43] S. Yamada, K. Nakayama, H. Takayama, *J. Org. Chem.* **1983**, *48*, 3477.
- [44] M. G. Zagorski, R. G. Salomon, *J. Am. Chem. Soc.* **1982**, *104*, 3498.
- [45] N. T. Kjer, H. Lund, *Acta Chem. Scand.* **1995**, *49*, 848.
- [46] S. Antonello, M. Musumeci, D. D. M. Wayner, F. Maran, *J. Am. Chem. Soc.* **1997**, *119*, 9541.
- [47] M. S. Workentin, F. Maran, D. D. M. Wayner, *J. Am. Chem. Soc.* **1995**, *117*, 2120.
- [48] R. L. Donkers, F. Maran, D. D. M. Wayner, M. S. Workentin, *J. Am. Chem. Soc.* **1999**, *121*, 7239.
- [49] R. L. Donkers, M. S. Workentin, *J. Phys. Chem.* **1998**, *102*, 4061.
- [50] R. L. Donkers, J. Tse, M. S. Workentin, *Chem. Commun.* **1999**, 135.
- [51] M. S. Workentin, R. L. Donkers, *J. Am. Chem. Soc.* **1998**, *120*, 2664.
- [52] D. D. M. Wayner, V. D. Parker, *Acc. Chem. Res.* **1993**, *26*, 287.
- [53] C. G. Moore, *J. Chem. Soc.* **1951**, 234.
- [54] A. C. Baldwin, *The Chemistry of Peroxides*, Wiley, New York, **1983**.
- [55] L. Batt, K. Kristie, R. T. Milne, A. Summers, *Int. J. Chem. Kinet.* **1974**, *6*, 877.
- [56] J.-M. Savéant in *Advances in Electron Transfer Chemistry* (Ed.: P. S. Mariano), JAI Press, Greenwich, CT, **1994**, p. 53.
- [57] C. P. Andrieux, I. Gallardo, J.-M. Savéant, K.-B. Su, *J. Am. Chem. Soc.* **1986**, *108*, 638.
- [58] J.-M. Savéant, *Acc. Chem. Res.* **1993**, *26*, 455.

- [59] S. Antonello, F. Maran, *J. Am. Chem. Soc.* **1998**, *120*, 5713.
[60] J.-M. Savéant, *J. Am. Chem. Soc.* **1987**, *109*, 6788.
[61] J.-M. Savéant, *J. Am. Chem. Soc.* **1992**, *114*, 10595.
[62] T. Lund, H. Lund, *Acta Chem. Scand. Ser. B.* **1987**, *41*, 93.
[63] C. Burkholder, W. R. Dolbier, Jr., M. Medebielle, *J. Org. Chem.* **1998**, *63*, 5385.
[64] C. P. Andrieux, D. Differding, M. Robert, J.-M. Savéant, *J. Am. Chem. Soc.* **1993**, *115*, 6592.
[65] S. Jakobsen, H. Jensen, S. U. Pedersen, K. Daasbjerg, *J. Phys. Chem.* **1999**, *103*, 4141.
[66] M. G. Severin, M. C. Arévalo, F. Maran, E. Vianello, *J. Phys. Chem.* **1993**, *97*, 150.
[67] T. B. Christensen, K. Daasbjerg, *Acta Chem. Scand.* **1997**, *51*, 307.
[68] K. Daasbjerg, H. Jensen, R. Benassi, F. Taddei, S. Antonello, A. Gennaro, F. Maran, *J. Am. Chem. Soc.* **1999**, *121*, 1750.
[69] *The Merck Index*, 11th ed. Merck Co. Inc., Rahway, NJ (USA), **1989**.
[70] J.-M. Savéant, D. Tessier, *Faraday Discuss. Chem. Soc.* **1982**, *74*, 57.
[71] A. J. Bard, L. R. Faulkner, *Electrochemical Methods, Fundamentals and Applications* Wiley, New York, **1980**.
[72] D. Brown, B. T. Davis, T. G. Halsall, A. R. Hands, *J. Chem. Soc.* **1962**, 4492.
[73] C. P. Andrieux, C. Blocman, J. M. Dumas-Bouchait, F. M'Halla, J.-M. Savéant, *Electroanal. Chem.* **1980**, *113*, 19.
[74] C. P. Andrieux, C. Blocman, J. M. Dumas-Bouchait, J.-M. Savéant, *J. Am. Chem. Soc.* **1979**, *101*, 3431.
[75] C. P. Andrieux, J.-M. Savéant, *Electroanal. Chem.* **1986**, *205*, 43.
[76] K. Daasbjerg, S. U. Pedersen, H. Lund, *Acta Chem. Scand.* **1991**, *45*, 424.
[77] S. U. Pedersen, K. Daasbjerg, *Acta Chem. Scand.* **1989**, *43*, 301.
[78] S. Antonello, F. Maran, *J. Am. Chem. Soc.* **1998**, *119*, 12595.
[79] F. Maran, D. D. M. Wayner, M. S. Workentin in *Advances in Physical Organic Chemistry* (Ed.: T. Tidwell), Academic Press, in press.
[80] S. Antonello, F. Maran, *J. Am. Chem. Soc.* **1999**, *121*, 9668.
[81] J. C. Imbeaux, J.-M. Savéant, *J. Electroanal. Chem.* **1973**, *44*, 169.
[82] H. J. V. Tyrrell, K. R. Harris, *Diffusion in Liquids*, Butterworths, London, **1984**.
[83] C. Erkey, A. Akgerman in *Measurements of the Transport Properties of Liquids* (Eds.: W. A. Wakeham, A. Nagashima, J. V. Sengers), Blackwell, London, **1991**, p. 251.
[84] E. D. German, A. M. Kuznetsov, *J. Phys. Chem. A* **1994**, *98*, 6120.
[85] H. Kojima, A. J. Bard, *J. Am. Chem. Soc.* **1975**, *97*, 6317.
[86] R. S. Brown, *Can. J. Chem.* **1975**, *53*, 3439.
[87] G. O. Schenck, *Angew. Chem.* **1952**, *64*, 12.
[88] W. Adam, H. J. Eggelte, *J. Org. Chem.* **1977**, *42*, 3987.
[89] R. F. Nystrom, W. G. Brown, *J. Am. Chem. Soc.* **1948**, *70*, 3738.
[90] E. C. Horning in *Synthesis of Azobenzene Vol. 3*, Wiley, London, **1955**, p. 103.
[91] W. McPherson, G. W. Stratton, *J. Am. Chem. Soc.* **1915**, *37*.

Received: January 18, 2001

Revised: May 21, 2001 [F3008]